Available online at www.sciencedirect.com
ScienceDirect
Journal of Colloid and Interface Science 301 (2006) 651–659
JOURNAL OF Colloid and Interface Science
www.elsevier.com/locate/jcis

Numerical calculation of the electrophoretic mobility of concentrated suspensions of soft particles

J.J. López-García [a], C. Grosse [b,c], J. Horno [a,*]

[a] Departamento de Física, Universidad de Jaén, Facultad de Ciencias Experimentales, Campus de las Lagunillas, Ed. A-3, 23071 Jaén, Spain
[b] Departamento de Física, Universidad Nacional de Tucumán, Av. Independencia 1800, 4000 San Miguel de Tucumán, Argentina
[c] Consejo Nacional de Investigaciones Científicas y Técnicas, Argentina

Received 23 February 2006; accepted 11 May 2006

Available online 20 May 2006

Abstract

The electrophoretic mobility of spherical soft particles in concentrated colloidal suspensions is numerically calculated. The particle is modeled as a hard core coated with an ion-penetrable membrane bearing a uniform distribution of fixed charges, while the high particle concentration is taken into account by means of a cell model. The network simulation method used makes it possible to solve the problem without any restrictions on the values of the parameters such as particle concentration, membrane thickness, fixed charge density in the membrane, viscous drag in the membrane, number and valence of ionic species, electrolyte concentration, etc. The theoretical model used is similar to the one presented by Ohshima [H. Ohshima, J. Colloid Interface Sci. 225 (2000) 233], except for the use of the Shilov–Zharkikh, rather than the Levine–Neale, boundary condition for the electric potential, and the inclusion in the force balance equation of an additional term corresponding to the force exerted by the liquid on the core of the moving particle [J.J. López-García, C. Grosse, J. Horno, J. Colloid Interface Sci. 265 (2003) 327]. The obtained results only coincide with existing analytical expressions for low particle concentrations, low particle charge, and when the electrolyte concentration is high, the membrane is thick, and its resistance to the fluid flow is high. This suggests that most interpretations of the electrophoretic mobility of soft particles in concentrated suspensions require numerical calculations.

Keywords: Electrophoretic mobility; Soft particle; Concentrated suspension; Network simulation method

1. Introduction

The theoretical model of suspended hard spherical particles and the associated boundary conditions [1,2] have been extended in recent years to more realistic physical situations, e.g., spherical particles with anomalous surface conductivity [3–5], spheroidal particles [6–9], spherical particles in concentrated suspensions [10,11], "soft" particles (hard particles coated with an ion-permeable membrane) [12–17], etc. Soft particles are particularly important in the study of many biological problems. For example, the peripheral zone of a human erythrocyte contains a charged glycoprotein layer and its surface structure can be estimated by electrophoresis. Several authors have developed theoretical models and have analyzed the behavior of dilute colloidal suspensions of soft particles. It is well known, nevertheless, that in most situations of practical interest involving biological systems, the suspensions are concentrated.

To our knowledge, only two studies of the electrokinetic properties of soft colloidal particles in concentrated suspensions [18,19] were published to date. However, the first presents semianalytical solutions with a range of validity that is limited to cases when the core radius tends to zero or when $\lambda(b-a) \gg 1$. Here b is the outer membrane radius, a is the core radius, and λ^2 is the ratio between the frictional coefficient of the membrane and the viscosity of the fluid. As for the second, it deals with a more complicated model that includes a charged core (actually, the considered parameter is the core potential). Unfortunately, the calculation corresponds to the case of a vanishing permittivity of the core, as is implied in Eq. (19) in [19] (see, for example, Eq. (4.23) in [20] or our Eq. (31)).

In this work we use the network simulation method [21] to obtain the electrophoretic mobility in concentrated colloidal

* Corresponding author.
E-mail address: jhorno@ujaen.es (J. Horno).

0021-9797/$ – see front matter
doi:10.1016/j.jcis.2006.05.035

suspensions of hard spherical particles coated with an ion-penetrable membrane bearing fixed charges, immersed in a general electrolyte solution. The network approach makes it possible to solve the problem without any restrictions on the values of the parameters such as thickness of the membrane, number of ionic species, fixed charge density in the membrane, etc.

Our model consists in a combination of a cell model, used to take into account the high particle concentration, and of a soft particle model, used to represent the charged ion-permeable membrane surrounding the hard core. For the cell model, the boundary conditions are fairly well established [11,18,22–25] except for the condition on the electric potential. The earlier works used the Levine–Neale condition [26] that was partly superseded in more recent works by the condition of Shilov–Zharkikh [27]. We prefer the latter on theoretical grounds [28], but also use the former for comparison.

As for the particle model, there are two possible representations of the fixed charge density of the polymer layer surrounding the particle: a continuous function that decreases monotonously with the distance to the core [15] or a constant value that drops to zero at a distance equal to the layer thickness [16,17]. The first approach has the advantage of generality (the shape of the density function can be modified by means of an additional parameter) and of avoiding the use of a boundary condition at the outer layer limit (which remains actually undefined). On the contrary, the second approach has the advantage of representing the system with the minimum number of parameters: the charge density of the polymer layer and its thickness. In this work we use this second model because it has the crucial advantage that the total charge of the polymer layer is completely contained within the unit cell volume.

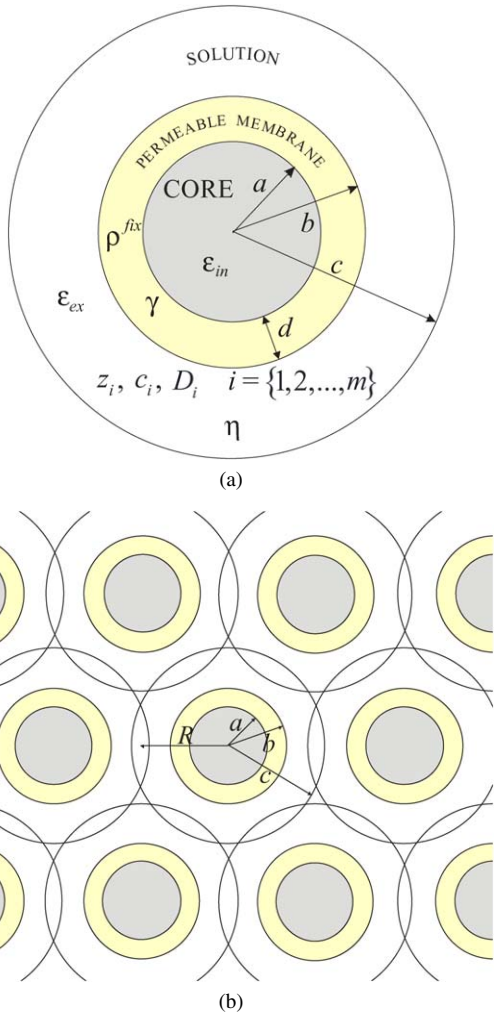

Fig. 1. Schematic representation of a spherical soft particle (a) and of a concentrated suspension using a cell model (b). a is the radius of the hard core, b the outer radius of the polyelectrolyte layer, and c the radius of the unit cell, Eq. (1). Note that, in view of this expression, c is larger than the average half distance R between neighboring particles ($c^3/R^3 = 3\sqrt{2}/\pi$ in the usual compact sphere packing representation used in the figure).

2. Theory

2.1. Description of the problem

Consider a concentrated suspension of charged spherical soft particles moving with an electrophoretic velocity v_e under the action of a DC electric field of strength E in a liquid containing a general electrolyte. We assume that the particle core of radius a is coated with an ion-penetrable layer of polyelectrolyte with thickness d. The particle has, therefore, an inner radius a and an outer radius $b = a + d$, Fig. 1a. We use a cell model [18] in which each particle is surrounded by a concentric spherical shell of electrolyte solution, having an outer radius c, such that the particle/cell volume ratio in the unit cell is equal to the particle volume fraction ϕ throughout the entire dispersion (Fig. 1b),

$$\phi = \left(\frac{b}{c}\right)^3. \tag{1}$$

The polyelectrolyte shell is uniformly charged with a total charge Q, and a volume charge density ρ^{fix}. On the other hand, the ionic solution is formed by m ionic species with charge numbers z_i ($i = 1, \ldots, m$), diffusion coefficients D_i, and bulk molar concentrations c_i^∞. Finally, the permittivity of the core is ε_{in} and that of the electrolyte solution is ε_{ex}. For sake of simplicity we consider that the permittivity of the polyelectrolyte layer and the ion diffusion coefficients inside that layer have the same values as in the electrolyte solution. The equations governing the dynamics of this system are well known [16]:

(a) *Nernst–Planck equations for the ionic fluxes*:

$$\vec{v}_i(\vec{r}) = -D_i \nabla \ln\bigl[c_i(\vec{r})\bigr] - \frac{z_i e D_i}{kT} \nabla\psi(\vec{r}) + \vec{v}(\vec{r}). \tag{2}$$

(b) *Continuity equations for each ionic species*:

$$\nabla \cdot \bigl[c_i(\vec{r})\vec{v}_i(\vec{r})\bigr] = 0. \tag{3}$$

(c) *Poisson equation*:

$$\nabla^2\psi(\vec{r}) = \begin{cases} -\dfrac{eN_A\sum_{i=1}^m z_i c_i(\vec{r})}{\varepsilon_{\text{ex}}} - \dfrac{\rho^{\text{fix}}}{\varepsilon_{\text{ex}}}, & a \leqslant r \leqslant b, \\ -\dfrac{eN_A\sum_{i=1}^m z_i c_i(\vec{r})}{\varepsilon_{\text{ex}}}, & b < r \leqslant c. \end{cases} \tag{4}$$

(d) *Navier–Stokes equation for a viscous fluid*:

$$-\eta\nabla^2\vec{v}(\vec{r}) + \nabla P(\vec{r}) + eN_A\left[\sum_{i=1}^m z_i c_i(\vec{r})\right]\nabla\psi(\vec{r})$$

$$+\rho_f\big[\vec{v}(\vec{r})\cdot\nabla\big]\vec{v}(\vec{r}) = \begin{cases} -\gamma\vec{v}(\vec{r}), & a \leqslant r \leqslant b, \\ 0, & b < r \leqslant c. \end{cases} \tag{5}$$

(e) *Continuity equation for an incompressible fluid*:

$$\nabla\cdot\vec{v}(\vec{r}) = 0, \tag{6}$$

where $\vec{v}_i(\vec{r})$ and $c_i(\vec{r})$ are, respectively, the velocity and the concentration (in $\mathrm{mol/m^3}$) of the ionic species i. The electric potential is represented by means of the symbol $\psi(\vec{r})$; $\vec{v}(\vec{r})$ is the fluid velocity, and $P(\vec{r})$ is the pressure. The constant e represents the elementary charge, while k, N_A, η, ρ_f, and T are, respectively, the Boltzmann constant, the Avogadro number, the fluid viscosity coefficient, the mass density of the fluid, and the absolute temperature of the system. Finally, γ is a parameter that represents the frictional coefficient exerted on the liquid flow by the polymer segments in the polyelectrolyte shell.

2.2. Linearization of the equations

In the absence of an applied electric field, there are no net forces acting on the particles and ions in the system, so that $\vec{v}(\vec{r})$ and $\vec{v}_i(\vec{r})$ $(i = 1, 2, \ldots, m)$ are all equal to zero, which transforms Eqs. (2), (4), and (5) into:

$$\nabla c_i^0(r) + \frac{z_i e}{kT} c_i^0(r)\nabla\psi^0(r) = 0, \tag{7}$$

$$\nabla^2\psi^0(r) = \begin{cases} -\dfrac{eN_A\sum_{i=1}^m z_i c_i^0(r)}{\varepsilon_{ex}} - \dfrac{\rho^{fix}}{\varepsilon_{ex}}, & a \leqslant r \leqslant b, \\ -\dfrac{eN_A\sum_{i=1}^m z_i c_i^0(r)}{\varepsilon_{ex}}, & b < r \leqslant c, \end{cases} \tag{8}$$

$$\nabla P^0(r) + eN_A\left[\sum_{i=1}^m z_i c_i^0(r)\right]\nabla\psi^0(r) = 0, \tag{9}$$

where $\psi^0(r)$, $P^0(r)$, and $c_i^0(r)$ are, respectively, the electric potential, the pressure and the concentration of the ionic species i in the absence of an applied electric field, i.e., when the system is in equilibrium (upper index "0").

The Nernst–Planck equations (7) can be easily solved, leading to the well-known Boltzmann distribution for the ionic concentrations:

$$c_i^0(r) = c_i^\infty \exp\left[-\frac{z_i e\psi^0(r)}{kT}\right]. \tag{10}$$

The integration constants c_i^∞ coincide with the bulk concentration values if the potential value $\psi^0(c)$ is chosen in such a way as to assure that the total charge inside the unit cell vanishes.

We now consider that a uniform DC electric field E is applied to the system. The meaning of E is that of the volume average of the microscopic electric field taken over the volume of the suspension. This way of doing does not coincide with Ohshima [18], who expresses his results in terms of an external field E_{ex}. Both field values can be defined considering that the space between the electrodes of a parallel plate condenser is filled with two slabs in series: one made of the suspension and the other of the electrolyte solution. Then, the potential drop across the suspension divided by its thickness is equal to E whereas the potential drop across the electrolyte solution divided by its thickness is equal to E_{ex}. While the physical problem can be correctly described using either of these two fields, our choice has the obvious advantage of being directly related to a measured quantity.

Under the action of the applied field, all the variables are perturbed around their equilibrium values, so that the ionic concentrations, the electric potential, and the pressure distributions can be expressed as a sum of their equilibrium values plus a perturbation term:

$$c_i(\vec{r}) = c_i^0(r) + \delta c_i(\vec{r}), \tag{11}$$

$$\psi(\vec{r}) = \psi^0(r) + \delta\psi(\vec{r}), \tag{12}$$

$$P(\vec{r}) = P^0(r) + \delta P(\vec{r}). \tag{13}$$

Under the assumption, fulfilled in most experimental determinations, that the applied field strength is sufficiently small so that all the induced ion concentration changes are small as compared to their equilibrium values, all the field-induced quantities of the problem are linear in E. This makes it possible to linearize the equation system by keeping only terms that are linear in the perturbations.

The resulting system can be further simplified combining the Nernst–Planck and Poisson equations in order to eliminate $\vec{v}_i(\vec{r})$ and taking the curl of the Navier–Stokes equation in order to eliminate the pressure change. Choosing a reference system with origin centered on the particle and polar axis in the direction of the applied field, the different variables can be written as explicit functions of the spherical coordinates:

$$\vec{v}_i(\vec{r}) = v_{ir}(r)\cos\theta\hat{e}_r + v_{i\theta}(r)\sin\theta\hat{e}_\theta, \tag{14}$$

$$\vec{v}(\vec{r}) = v_r(r)\cos\theta\hat{e}_r + v_\theta(r)\sin\theta\hat{e}_\theta, \tag{15}$$

$$\vec{\Omega}(\vec{r}) = \Omega(r)\sin\theta\hat{e}_\varphi, \tag{16}$$

$$\delta c_i(\vec{r}) = \delta c_i(r)\cos\theta, \tag{17}$$

$$\delta\psi(\vec{r}) = \delta\psi(r)\cos\theta. \tag{18}$$

where $\hat{e}_r$, $\hat{e}_\theta$, and $\hat{e}_\varphi$ are the unit vectors and

$$\vec{\Omega}(\vec{r}) = \nabla\times\vec{v}(\vec{r}) \tag{19}$$

is the vorticity. This transforms the equation system into:

$$\begin{aligned} &\frac{1}{r^2}\frac{d}{dr}\left\{r^2\frac{d}{dr}\left[\frac{\delta c_i(r)}{c_i^0(r)} + \frac{z_i e\delta\psi(r)}{kT}\right]\right\} \\ &\quad - \frac{2}{r^2}\left[\frac{\delta c_i(r)}{c_i^0(r)} + \frac{z_i e\delta\psi(r)}{kT}\right] \\ &\quad - \frac{z_i e}{kT}\frac{d\psi^0(r)}{dr}\frac{d}{dr}\left[\frac{\delta c_i(r)}{c_i^0(r)} + \frac{z_i e\delta\psi(r)}{kT}\right] \\ &= -\frac{z_i e}{kT}\frac{d\psi^0(r)}{dr}\frac{v_r(r)}{D_i}, \end{aligned} \tag{20}$$

$$\frac{1}{r^2}\frac{d}{dr}\left[r^2\frac{d\delta\psi(r)}{dr}\right] - \frac{2\delta\psi(r)}{r^2} = -\frac{eN_A\sum_{i=1}^m z_i\delta c_i(r)}{\varepsilon_{ex}}, \tag{21}$$

$$\Omega(r) = \frac{v_r(r) + v_\theta(r)}{r} + \frac{dv_\theta(r)}{dr}, \tag{22}$$

$$\frac{d^2\Omega(r)}{dr^2} + \frac{2}{r}\frac{d\Omega(r)}{dr} - \frac{2\Omega(r)}{r^2}$$

$$-\frac{eN_A}{\eta r}\frac{d\psi^0(r)}{dr}\sum_{i=1}^{m}\left\{z_i c_i^0(r)\left[\frac{\delta c_i(r)}{c_i^0(r)}+\frac{z_i e\delta\psi(r)}{kT}\right]\right\} = \begin{cases}\frac{\gamma}{\eta}\Omega(r), & a\leqslant r\leqslant b,\\ 0, & b<r\leqslant c,\end{cases} \tag{23}$$

$$\frac{2[v_r(r)+v_\theta(r)]}{r}+\frac{dv_r(r)}{dr}=0. \tag{24}$$

2.3. Boundary conditions

The following boundary conditions over the outer surface of the unit cell ($r=c$), at the membrane-electrolyte solution interface ($r=b$), and at the particle core ($r=a$), must be satisfied by each variable of interest. Most of these conditions have been extensively used in preceding works involving cell-models and/or soft particle models. We shall just write down these conditions. In contrast, we shall briefly discuss those conditions that differ from previous calculations.

2.3.1. Electric potential

At $r=c$, the equilibrium potential must satisfy the condition of electroneutrality of the whole unit cell. Therefore, in view of the Gauss law:

$$\left.\frac{d\psi^0(r)}{dr}\right|_{r=c^-}=0. \tag{25}$$

At $r=a$, the gradient of the equilibrium potential is determined by the net charge of the core. In this work we consider that the core is uncharged, so that:

$$\left.\frac{d\psi^0(r)}{dr}\right|_{r=a^+}=0. \tag{26}$$

The volume average of the electric field calculated over the unit cell must be equal to the macroscopic field in the suspension:

$$\frac{\int_{V_c}\nabla\psi(\vec{r})\,dV}{V_c}=\frac{\int_{S_c}\psi(c)\hat{e}_r\,dS}{V_c} =-\frac{2\pi\int_0^\pi\delta\psi(c)\cos^2\theta c^2\sin\theta\,d\theta}{4\pi c^3/3} =\frac{\delta\psi(c)}{c}=-E, \tag{27}$$

where V_c is the volume of the unit cell and S_c is its surface. This is the Shilov–Zharkikh [27] boundary condition used in [11,25], which does not coincide with the condition of Levine–Neale [26]:

$$\left.\frac{d\delta\psi(r)}{dr}\right|_{r=c^-}=-E_{ex} \tag{28}$$

that was used by Ohshima [18] and also in [19,22–24]. Note that Eq. (28) is expressed in terms of E_{ex} rather than E.

At the membrane-electrolyte solution interface, the boundary conditions are the continuity of the electric potential and the continuity of the normal component of the displacement vector:

$$\delta\psi(b^-)=\delta\psi(b^+), \tag{29}$$

$$\left.\frac{d\delta\psi(r)}{dr}\right|_{r=b^-}=\left.\frac{d\delta\psi(r)}{dr}\right|_{r=b^+}. \tag{30}$$

Finally, the boundary condition at the surface of the core is obtained from the continuity of the electric potential and that of the normal component of the displacement vector, together with the condition that the field inside the core is uniform and that $\delta\psi(0)$ must be zero by symmetry:

$$\left.\frac{d\delta\psi(r)}{dr}\right|_{r=a^+}=\frac{\varepsilon_{in}}{\varepsilon_{ex}}\frac{\delta\psi(a^+)}{a}. \tag{31}$$

2.3.2. Fluid velocity

Since the reference system is centered on the particle, the velocity of the liquid phase at the outer surface of the unit cell must be equal to minus the electrophoretic velocity v_e of the particle:

$$v_r(c^-)=-v_e. \tag{32}$$

This boundary condition, used in [11,18,22,23,25], is common to both the Kuwabara [29] and Happel [30] cell models, which differ in the second boundary condition as noted later.

At the membrane-electrolyte solution interface, the boundary conditions are the continuity of the radial and the tangential components of the velocity

$$v_r(b^-)=v_r(b^+), \tag{33}$$

$$v_\theta(b^-)=v_\theta(b^+). \tag{34}$$

In view of the fluid incompressibility, Eq. (24), condition (34) is equivalent to the continuity of the first derivative of the radial component of the fluid velocity:

$$\left.\frac{dv_r(r)}{dr}\right|_{r=b^-}=\left.\frac{dv_r(r)}{dr}\right|_{r=b^+}. \tag{35}$$

At the surface of the core, the velocity of the fluid must vanish due to its viscosity (adherence condition):

$$v_r(a^+)=0, \tag{36}$$

$$v_\theta(a^+)=0. \tag{37}$$

Using the incompressibility condition (24), expression (37) transforms to:

$$\left.\frac{dv_r(r)}{dr}\right|_{r=a^+}=0. \tag{38}$$

2.3.3. Ionic concentrations

At the outer surface of the unit cell, the perturbations of the ionic concentrations must vanish:

$$\delta c_i(c^-)=0. \tag{39}$$

This condition used in [11,18,19,23,25], is related to the requirement that the perturbation of the concentration at the mid point between two particles aligned with the field must be zero by symmetry. In some works [24] a different condition is used:

$$\left.\frac{d\delta c_i}{dr}\right|_{r=c^-}=0. \tag{40}$$

We prefer the former, because it does not exclude the diffusive ion flow across the unit cell boundary.

At the membrane-electrolyte solution interface, the ionic concentrations must be continuous:

$$\delta c_i(b^-) = \delta c_i(b^+). \tag{41}$$

Furthermore, the radial component of the ion velocities must be continuous:

$$v_{ir}(b^-) = v_{ir}(b^+) \tag{42}$$

which, combined with the linearized Nernst–Planck equations and Eq. (33), leads to

$$\left.\frac{d}{dr}\left[\frac{\delta c_i(r)}{c_i^0(r)} - \frac{z_i e\delta\psi(r)}{kT}\right]\right|_{r=b^-} = \left.\frac{d}{dr}\left[\frac{\delta c_i(r)}{c_i^0(r)} - \frac{z_i e\delta\psi(r)}{kT}\right]\right|_{r=b^+}. \tag{43}$$

Finally, the boundary condition over the core is determined by the requirement that ions cannot penetrate into it

$$v_{ir}(a^+) = 0 \tag{44}$$

which, combined with Nernst–Planck equations and Eq. (36), leads to

$$\left.\frac{d}{dr}\left[\frac{\delta c_i(r)}{c_i^0(r)} - \frac{z_i e\delta\psi(r)}{kT}\right]\right|_{r=a^+} = 0. \tag{45}$$

2.3.4. Vorticity

At the outer surface of the unit cell, the vorticity must vanish:

$$\Omega(c^-) = 0. \tag{46}$$

This is the second Kuwabara boundary condition, used in [11,18,19,22–25], which does not coincide with the second Happel condition, also used in [24], that considers that the shear stress of the fluid is zero:

$$\left.\eta\left[\frac{1}{r}\frac{\partial v_r\cos\theta}{\partial\theta} + r\frac{\partial}{\partial r}\left(\frac{v_\theta\sin\theta}{r}\right)\right]\right|_{r=c^-} = -\eta\frac{\sin\theta}{c}\left[v_r(c^-) + v_\theta(c^-)\right] = 0. \tag{47}$$

Again, we chose Eq. (46) rather than Eq. (47) on theoretical grounds (the Happel model does not reduce to the Smoluchowski result [22,26]).

At the membrane-electrolyte solution interface the tangential stress in the fluid must be continuous:

$$\left(\tau\cdot\hat{e}_r\right)\times\hat{e}_r\big|_{r=b^-} = \left(\tau\cdot\hat{e}_r\right)\times\hat{e}_r\big|_{r=b^+}, \tag{48}$$

where τ is the hydrodynamic stress tensor. This equation leads to the continuity of $\tau_{r\theta}$:

$$\left.\eta\left[\frac{dv_\theta(r)}{dr} + \frac{1}{2}\frac{dv_r(r)}{dr}\right]\sin\theta\right|_{r=b^-} = \left.\eta\left[\frac{dv_\theta(r)}{dr} + \frac{1}{2}\frac{dv_r(r)}{dr}\right]\sin\theta\right|_{r=b^+} \tag{49}$$

which shows, together with Eq. (35), that the derivative of the tangential component of the velocity is continuous. Combining this result with Eqs. (22), (33), and (34), leads to the continuity of the vorticity:

$$\Omega(b^-) = \Omega(b^+). \tag{50}$$

A second condition can be obtained evaluating the tangential component of the linearized Navier–Stokes equation at $r = b^-$:

$$\frac{\eta}{b}\frac{d}{dr}\left[r\Omega(r)\right]\Big|_{r=b^-} + \frac{\delta P(b^-)}{b} + eN_A\sum_{i=1}^{m} z_i c_i^0(b^-)\frac{\delta\psi(b)}{b} - \gamma v_\theta(b) = 0 \tag{51}$$

and at $r = b^+$:

$$\frac{\eta}{b}\frac{d}{dr}\left[r\Omega(r)\right]\Big|_{r=b^+} + \frac{\delta P(b^+)}{b} + eN_A\sum_{i=1}^{m} z_i c_i^0(b^+)\frac{\delta\psi(b)}{b} = 0. \tag{52}$$

Taking into account Eqs. (29) and (50), together with the continuity of the pressure [14] and the relation of the equilibrium ionic concentrations inside and outside of the membrane at $r = b$, leads to the condition:

$$\left.\frac{d\Omega(r)}{dr}\right|_{r=b^-} - \frac{\gamma}{\eta}v_\theta(b) + \frac{eN_A}{\eta}\sum_{i=1}^{m} z_i c_i^0(b)\frac{\delta\psi(b)}{b} = \left.\frac{d\Omega(r)}{dr}\right|_{r=b^+}. \tag{53}$$

According to the second law of Newton, the net force acting on the particle (the electric force acting on the fixed charges in the membrane $\vec{F}_e$ plus the mechanical force $\vec{F}_m$ acting on the particle) must vanish in the steady state, i.e.,

$$\vec{F}_e + \vec{F}_m = 0. \tag{54}$$

The mechanical force is made of two terms that correspond to the force exerted by the fluid on the membrane and on the surface of the core:

$$\vec{F}_m = \int_{V_m}\gamma\vec{v}(\vec{r})\,dV + \int_{S_p}\tau\cdot d\vec{S}, \tag{55}$$

where V_m is the volume of the membrane and S_p the surface of the core. As already noted in [16], the second addend in the right hand side of this equation is omitted in the theory of Ohshima, where it is assumed that the viscous force is only due to the integral over the volume occupied by the polyelectrolyte, as is the case for spherical polyelectrolytes.

Using Eqs. (15), (22), (24), (36), and (37) and the tangential component of the linearized Navier–Stokes equation, transforms Eq. (55) into:

$$F_m = \frac{4\pi}{3}\gamma b^3 v_r(b) + \frac{4\pi}{3}a^2\left[\eta a\left.\frac{d\Omega(r)}{dr}\right|_{r=a} - \eta\Omega(a) + eN_A\sum_{i=1}^{m} z_i c_i^0(a)\delta\psi(a)\right]. \tag{56}$$

Table 1

$a = 10^{-7}$ m	$d = 10^{-8}$ m	$D_1 = D_2 = 2 \times 10^{-9}$ m^2/s
$z_1 = -z_2 = 1$	$\varepsilon_{ex}/\varepsilon_0 = 78.5$	$\varepsilon_{in}/\varepsilon_0 = 2$
$T = 298$ K	$\eta = 8.9 \times 10^{-4}$ poise	$\rho^{fix} = 10^6$ C/m^3
$c_1^\infty = c_2^\infty = 1$ mol/m^3	$\kappa a = 10.39$	$\lambda a = 1$

On the other hand, the electrical force corresponds to the force exerted on the particle by the volume charge in the membrane:

$$F_e = -\rho^{fix} \int_a^b \int_0^\pi \left[\frac{d\delta\psi(r)}{dr} \cos^2\theta + \frac{\delta\psi(r)}{r} \sin^2\theta \right] \times 2\pi r^2 \sin\theta \, dr \, d\theta = -\frac{4\pi}{3} \rho^{fix} \left[b^2 \delta\psi(b) - a^2 \delta\psi(a) \right] \quad (57)$$

so that the boundary condition (54) for the vorticity over the core of the particle is, finally:

$$-\rho^{fix} \left[b^2 \delta\psi(b) - a^2 \delta\psi(a) \right] + \gamma b^3 v_r(b) + a^2 \left[\eta a \frac{d\Omega(r)}{dr}\bigg|_{r=a} - \eta\Omega(a) + eN_A \sum_{i=1}^{m} z_i c_i^0(a) \delta\psi(a) \right] = 0. \quad (58)$$

3. Results and discussion

The first step in the numerical procedure consists in the transformation of the equation system using dimensionless variables. An electrical circuit with the same governing differential equations is then designed. This is done dividing the unit cell into N compartments or volume elements, small enough for the spatial variations of all the variables to be linear within each compartment. Finally, an electric simulation program is used to obtain the values of the desired quantities, mainly currents and potentials at different positions of the circuit. The whole procedure, the discretized equations and the resulting circuit are presented in [16].

In what follows, we present the obtained numerical results for the dimensionless electrophoretic mobility, defined as

$$\tilde{u}_e = \frac{3e\eta}{2\varepsilon_{ex} kT} \frac{v_e}{E} \quad (59)$$

calculated for different situations. In view of the great number of parameters characterizing the system, it is not possible to analyze all the dependencies. We therefore considered as a starting point the system characterized by the parameters appearing in Table 1, and studied the dependencies with the electrolyte concentration, the membrane drag coefficient, the fixed charge density, and the volume fraction. When possible, we also compared our results with previous works.

Fig. 2 shows the dependence of the electrophoretic mobility on the electrolyte concentration (actually κa) for two limiting values of the drag coefficient ($\lambda a = 0$ and 100) and for different values of the volume fraction ϕ. This figure is similar to Fig. 5 in [16]: the upper ($\lambda a = 0$, $\phi = 0$) and one before the lower ($\lambda a = 100$, $\phi = 0$) curves of that figure are also present

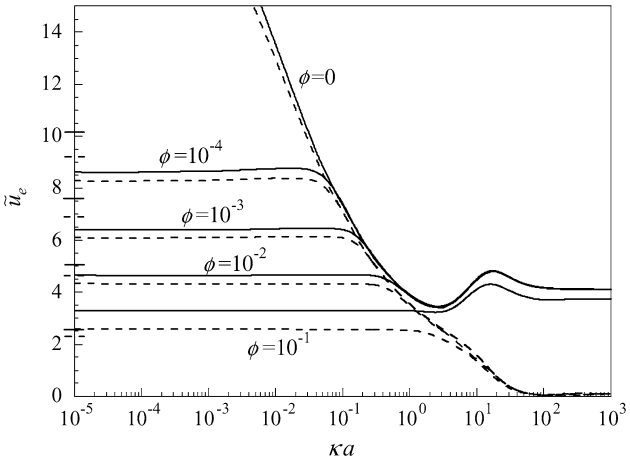

Fig. 2. Dependence of the electrophoretic mobility on the electrolyte concentration calculated for $\lambda a = 0$ (continuous lines) and $\lambda a = 100$ (dashed lines), and for different values of the volume fraction ϕ. The remaining parameters are given in Table 1. The line segments on the ordinate axis represent limiting values corresponding to a salt-free medium according to [31], Eq. (61).

in Fig. 2. The main difference between these figures arises at very low electrolyte concentrations: for $\kappa a \to 0$ and $\phi = 0$ the mobility curve strongly increases up to the limit given by the Stokes law in an insulating liquid, Eqs. (112) and (113) in [16]:

$$\tilde{u}_e = \begin{cases} \frac{e(b^3 - a^3)\rho^{fix}}{3\varepsilon_{ex} kT a}, & \lambda a = 0, \\ \frac{e(b^3 - a^3)\rho^{fix}}{3\varepsilon_{ex} kT b}, & \lambda a \to \infty. \end{cases} \quad (60)$$

For small but finite values of ϕ, however, the mobility values reach a plateau at much larger values of κa. This happens due to the electroneutrality condition in the unit cell: a further decrement of the electrolyte concentration at constant ϕ weakly changes the ion surrounding of the particle. Therefore, the electrophoretic mobility values should tend to their corresponding salt-free limit, when the particle is surrounded by the counterions and there are no co-ions in the system. The line segments crossing the ordinate axis correspond to these limiting values according to the Ohshima expression (Eqs. (35) and (36) in [31]):

$$\tilde{u}_e = \begin{cases} \frac{b}{a} \ln\left(\frac{1}{\phi}\right), & \lambda a = 0, \\ \ln\left(\frac{1}{\phi}\right), & \lambda a \to \infty. \end{cases} \quad (61)$$

It should be noted that these expressions are valid when the charge of the particle is relatively high:

$$Q > \frac{4\pi\varepsilon_{ex} bkT}{e} \ln\left(\frac{1}{\phi}\right). \quad (62)$$

This condition is very well satisfied in all the considered cases. The second condition: $\phi \ll 1$, is also well satisfied in all cases except for the highest volume fraction, $\phi = 0.1$.

The dependence of the electrophoretic mobility on the charge of the particle, calculated for $\kappa a = 10.39$, two values of the product λa ($\lambda a = 1$ and 100), and different values of the volume fraction ϕ, is presented in Fig. 3. In all cases, the membrane thickness is $d = 10^{-8}$ m, so that the two curves corresponding to $\phi = 0$ coincide with the fourth line in Fig. 6 and

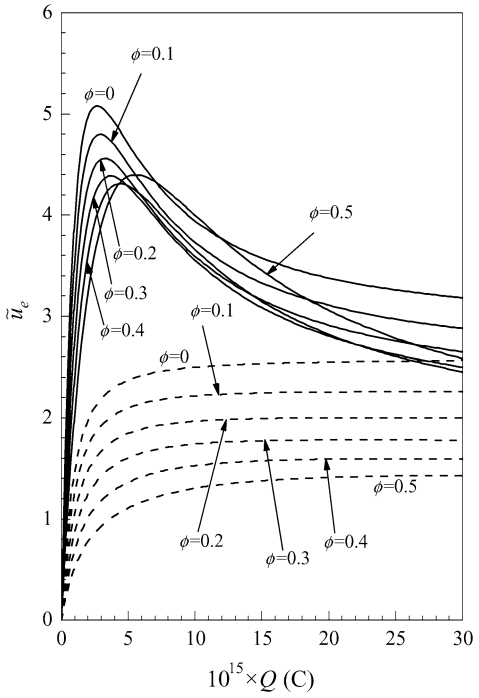

Fig. 3. Dependence of the electrophoretic mobility on the charge of the particle Q calculated for $\lambda a = 1$ (continuous lines) and $\lambda a = 100$ (dashed lines), and different values of the volume fraction ϕ. The remaining parameters are given in Table 1.

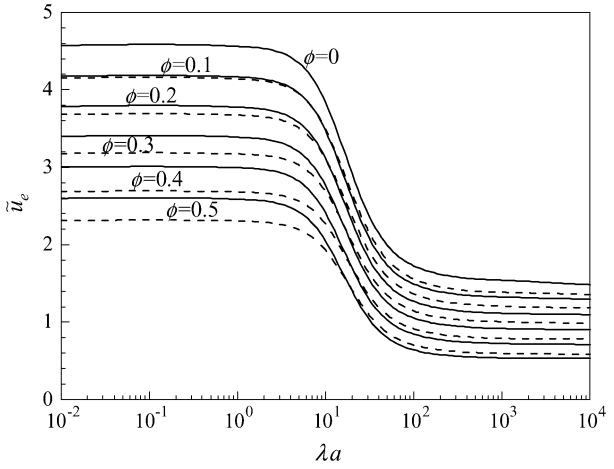

Fig. 4. Dependence of the electrophoretic mobility on the product λa calculated for different values of the volume fraction ϕ. Numerical results obtained using the Shilov–Zharkikh (continuous lines) and the Levine–Neale (dashed lines) boundary conditions. The remaining data are given in Table 1.

with the third continuous line in Fig. 7 of [16]. The dependence of the different curves on the charge of the particle is qualitatively similar to the dependence of the electrophoretic mobility of hard particles on the ζ potential [32]. However, the charge of the particle was used as independent variable in Fig. 3 because the ζ potential is not a well defined magnitude for soft particles [33].

In this figure, the set of continuous curves corresponds to $\lambda a = 1$ while the dashed curves correspond to $\lambda a = 100$. As expected, the electrophoretic mobility always decreases with increasing drag coefficient value. It also generally decreases with the volume fraction ϕ, but there appears to be an exception to this behavior for low values of λa and medium values Q. While an analysis of the electric potential, ion concentration, and fluid velocity profiles across the unit cell seem to be necessary to properly explain this behavior, two comments are in order. First: for very high values of the particle charge, higher than the maximum shown in Fig. 3, all the mobility values monotonously decrease with increasing volume fraction. Second: the non-monotonous dependence of the electrophoretic mobility on the volume fraction does not appear if the Levine–Neale boundary condition is used. However, it is important to keep in mind that the mobility values obtained using the two considered boundary conditions are not directly comparable (see comments of Fig. 4).

A comparison with the results obtained by Ohshima [18] is not immediate due to two main reasons:

1. The boundary condition for the electric potential used in [18] is that of Levin–Neale [26] and the mobility is calculated as v_e/E_{ex}. In contrast, we use the condition of Shilov–Zharkikh [27] and calculate the mobility as v_e/E. Therefore, the two mobility values are not directly comparable, except for $\phi \to 0$. Because of this, we were forced to recalculate our results using the Levine–Neale boundary condition.
2. The analytical expressions presented in [18] were deduced assuming that the following conditions are simultaneously met:

$$\lambda a \gg 1, \qquad \lambda d \gg 1, \qquad \kappa a \gg 1, \qquad \kappa d \gg 1. \tag{63}$$

The most restrictive requirement is the last one, which limits any comparison to particles with thick polyelectrolyte layers.

Fig. 4 shows the influence of the electric potential boundary condition and of the definition used for the electrophoretic mobility, on numerical values of u_e calculated as a function of λa for different values of the volume fraction ϕ. The continuous curves were obtained using the Shilov–Zharkikh boundary condition, while the Levine–Neale condition was used to calculate the dashed curves. For both sets, the numerical results corresponding to $\lambda a \to 0$ tend to a constant mobility value that is higher than for $\lambda a \to \infty$ because, in the first limit, the viscous drag acts only on the core while, in the second, it acts on the external surface of the polyelectrolyte layer.

As expected, both calculations overlap for $\phi = 0$ and the difference between results obtained using the two boundary conditions increases with ϕ. It is interesting to note that there is a crossover between these curves: the highest mobility is obtained using the Shilov–Zharkikh condition when λa is low while, for high λa, the Levine–Neale condition leads to the highest mobility. This behavior is related to the definition of the mobility as the electrophoretic velocity v_e divided by the macroscopic field E, in the case of the Shilov–Zharkikh condition, or the external field E_{ex}, when the Levine–Neale condition is used [18]. These two fields are related by the continuity of the electric cur-

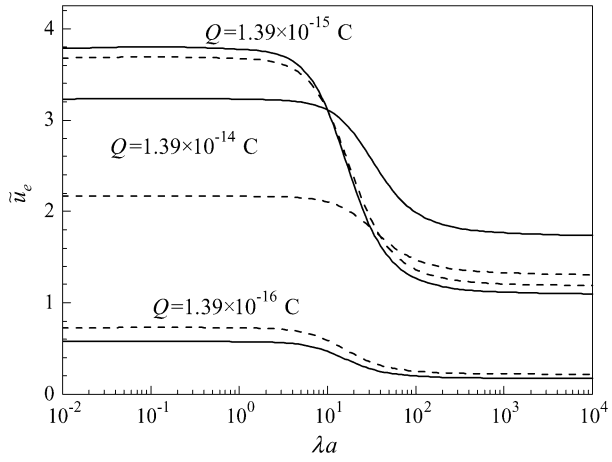

Fig. 5. As for Fig. 4, but calculated for $\phi = 0.2$ and for the indicated values of the charge of the particle Q.

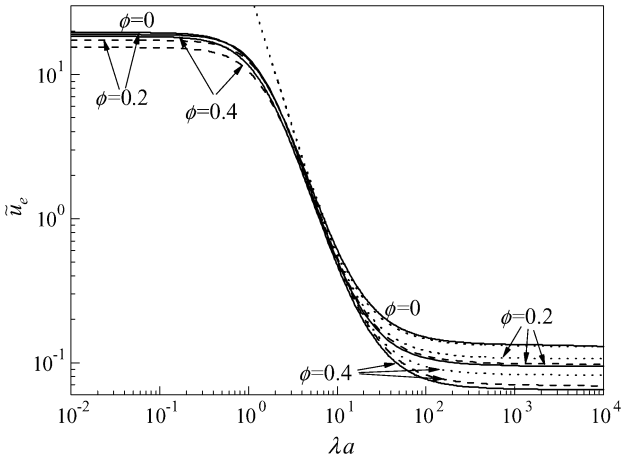

Fig. 6. Dependence of the electrophoretic mobility on the product λa calculated for different values of the volume fraction ϕ. Numerical results obtained using the Shilov–Zharkikh (continuous lines) and the Levine–Neale (dashed lines) boundary conditions, and analytical results of Ohshima [18] (dotted lines). The remaining parameters are given in Table 1, except for the value $d = a$ used in view of the fourth condition in Eq. (63).

rent density [1]:

$$K_s E = K_{ex} E_{ex}, \tag{64}$$

where K_s and K_{ex} represent the conductivities of the suspension and of the electrolyte solution, respectively. This suggests that the observed crossover of the mobility curves arises because the conductivity of the suspension is higher than that of the electrolyte solution for low values of λa, while K_s becomes lower than K_{ex} when the drag coefficient increases ($\lambda a \to \infty$).

This interpretation is confirmed in Fig. 5, which shows the results obtained for a single concentration $\phi = 0.2$ and three values of the charge of the particle: $Q = 1.39 \times 10^{-16}$, 1.39×10^{-15}, and 1.39×10^{-14} C. As can be seen, for the lowest charge value, the conductivity of the suspension appears to be lower than that of the electrolyte solution, irrespective of the λa value, so that the Shilov–Zharkikh line lies entirely below the Levine–Neale curve. The opposite occurs for the highest Q value, for which the conductivity of the suspension appears to be higher than that of the electrolyte solution in the whole λa range. This qualitative behavior of the two numerical solutions and its relationship to the conductivity of the suspension can also be observed for hard particles (Figs. 3 and 4 in [11]).

A comparison between our numerical calculations and the analytical results (Eq. (4.26) in [18]) is presented in Fig. 6. In view of the fourth condition in Eq. (63), particles with thick double layer $d = a$ had to be considered. The dotted curves correspond to the analytical expression of Ohshima, the continuous curves to numerical calculation using the Shilov–Zharkikh boundary condition, and the dashed curves to calculations using the condition of Levine–Neale. The upper curves were calculated for $\phi = 0$, so that the two numerical results overlap (these curves coincide with the lowest curves in Fig. 8 in [16]). As can be seen, for $\phi = 0$, the agreement between the numerical and analytical results is excellent for high values of λa, but rapidly deteriorates for decreasing values of this parameter. For $\lambda a \to 0$ the analytical results diverge since, in view of the boundary condition used, the viscous drag is only due to the polyelectrolyte layer and vanishes, therefore, in this limit. It should be noted, however that according to the first requirement of Eq. (63), the analytical expression should not be used for low values of λa.

When the volume fraction is increased, the agreement between theoretical and numerical results becomes much worse than for $\phi = 0$, even in the limit $\lambda a \to \infty$. Actually, the two numerical curves are much closer to one another than to the theoretical curve. A possible reason for this behavior is, again, the boundary condition used in the theoretical model [18], that omits the viscous drag on the core of the particle. When the particle concentration increases, more fluid is forced to flow inside the polyelectrolyte layer, increasing the consequences of this omission.

This limiting behavior is further analyzed in Fig. 7, where the numerical results are compared to the theoretical predictions as a function of the volume fraction for three values of the charge of the particle. Also included is a theoretical curve corresponding to the definition v_e/E for the electrophoretic mobility, which was obtained combining Eq. (4.26) in [18] with a theoretical expression for the quotient K_s/K_{ex}: Eq. (31) in [34]. This last expression is restricted to all the requirements in Eq. (63) and, additionally, to low values of the Donnan potential. This is why it could only be calculated for the lowest value of the fixed charge. As can be seen, important deviations with respect to both numerical calculations appear for high concentrations and for highly charged particles.

All of the above raises some reservations on the use of the existing analytical expression for the interpretation of experimental data for the electrophoretic mobility of soft particles in concentrated suspensions. Firstly because of the stringent requirements for the validity of the analytical expression, Eq. (63), which limit its applicability to particles with thick membrane and relatively high drag coefficient. Then because of the definition of the electrophoretic mobility given in terms of the external field, when the experimentally accessible value

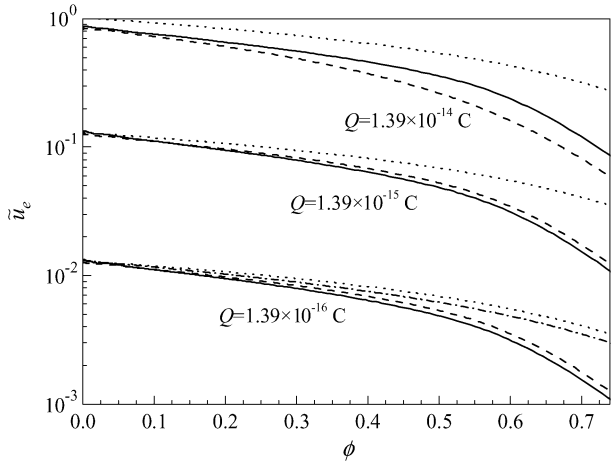

Fig. 7. Dependence of the electrophoretic mobility on the volume fraction ϕ calculated for the indicated values of the charge of the particle Q. Numerical results obtained using the Shilov–Zharkikh (continuous lines) and the Levine–Neale (dashed lines) boundary conditions, analytical results of Ohshima [18] (dotted lines), and analytical results of Ohshima [18] combined with an analytical expression for K_s/K_{ex} [34] in order to express the electrophoretic mobility in terms of E rather than E_{ex} (dash and point line). The remaining parameters are given in Table 1, except for the values $d = a$, used in view of the fourth condition in Eq. (63), and $\lambda a = 10^4$, highest value in Fig. 6.

is that of the macroscopic field (an analytical expression relating both fields is only available for weakly charged particles: [34] and Eq. (64)). Finally, because even when all the conditions stated for the validity of Eq. (63) are met, the approximate analytical solution of the integral equations presents substantial deviations from numerical results, except for low concentrations of weakly charged particles. This suggests that most interpretations of the electrophoretic mobility of soft particles in concentrated suspensions require numerical calculations.

Acknowledgments

Financial support by Ministerio de Ciencia y Tecnología (BFM2003-4856) and Consejería de Innovación, Ciencia y Empresa de la Junta de Andalucía (project FQM 410) of Spain, Consejo de Investigaciones de la Universidad Nacional de Tucumán (26/E220) and Consejo Nacional de Investigaciones Científicas y Técnicas (PIP 0465/98) of Argentina is gratefully acknowledged.

References

[1] S.S. Dukhin, V.N. Shilov, Dielectric Phenomena and the Double Layer in Disperse Systems and Polyelectrolytes, Kerter Publishing House, Jerusalem, 1974.
[2] E.H.B. DeLacey, L.R. White, J. Chem. Soc. Faraday Trans. 2 77 (1981) 2007.
[3] M. Minor, A. van der Wal, J. Lyklema, in: E. Pelizetti (Ed.), Fine Particles Science and Technology, Kluwer Academic, Dordrecht/Norwell, MA, 1996, pp. 225–238.
[4] C.S. Mangelsdorf, L.R. White, J. Chem. Soc. Faraday Trans. 94 (1998) 2441.
[5] R.J. Hunter, Adv. Colloid Interface Sci. 100 (2003) 153.
[6] R.W. O'Brien, D.N. Ward, J. Colloid Interface Sci. 121 (1988) 402.
[7] B.J. Yoon, S. Kim, J. Colloid Interface Sci. 128 (1989) 275.
[8] H.J. Keh, T.Y. Huang, J. Colloid Interface Sci. 160 (1993) 354.
[9] A.J. Poza, J.J. Lopez-García, A. Hayas, J. Horno, J. Colloid Interface Sci. 219 (1999) 241.
[10] A.S. Dukhin, V. Shilov, Y. Borkovskaya, Langmuir 15 (1999) 3452.
[11] F. Carrique, F.J. Arroyo, A.V. Delgado, J. Colloid Interface Sci. 243 (2001) 351.
[12] H. Ohshima, J. Colloid Interface Sci. 163 (1994) 474.
[13] J.J. López-García, J. Horno, C. Grosse, Phys. Chem. Chem. Phys. 3 (2001) 3754.
[14] H. Ohshima, J. Colloid Interface Sci. 228 (2000) 190.
[15] R.J. Hill, D.A. Saville, W.B. Russel, J. Colloid Interface Sci. 258 (2003) 56.
[16] J.J. López-García, C. Grosse, J. Horno, J. Colloid Interface Sci. 265 (2003) 327.
[17] J.J. López-García, C. Grosse, J. Horno, J. Colloid Interface Sci. 265 (2003) 341.
[18] H. Ohshima, J. Colloid Interface Sci. 225 (2000) 233.
[19] E. Lee, K. Chou, J. Hsu, J. Colloid Interface Sci. 280 (2004) 518.
[20] C.S. Mangelsdorf, L.R. White, J. Chem. Soc. Faraday Trans. 88 (1992) 3567.
[21] J.J. López-García, J. Horno, in: J. Horno (Ed.), Network Simulation Method, Research Signpost, Trivandrum, 2002.
[22] T.J. Johnson, E.J. Davis, J. Colloid Interface Sci. 215 (1999) 397.
[23] E. Lee, J.W. Chu, J.P. Hsu, J. Colloid Interface Sci. 209 (1999) 240.
[24] J.M. Ding, H.J. Keh, J. Colloid Interface Sci. 236 (2001) 180.
[25] F. Carrique, F.J. Arroyo, M.L. Jimenez, A.V. Delgado, J. Phys. Chem. B 107 (2003) 3199.
[26] S. Levine, G.H. Neale, J. Colloid Interface Sci. 47 (1974) 520.
[27] V.N. Shilov, N.I. Zharkikh, Y.B. Borkovskaya, Colloid J. 43 (1981) 434.
[28] A.S. Dukhin, V.N. Shilov, Y.B. Borkovskaya, Langmuir 15 (1999) 3452.
[29] S. Kuwabara, J. Phys. Soc. Jpn. 14 (1959) 527.
[30] J. Happel, AIChE J. 4 (1958) 197.
[31] H. Ohshima, J. Colloid Interface Sci. 269 (2004) 255.
[32] R.W. O'Brien, L.R. White, J. Chem. Soc. Faraday Trans. 2 74 (1978) 1607.
[33] H. Ohshima, in: A.T. Hubbard (Ed.), Encyclopedia of Surface and Colloid Science, vol. 2, Dekker, New York, 2002.
[34] H. Ohshima, J. Colloid Interface Sci. 229 (2000) 307.